Journal of Metals, Materials and Minerals. Vol. 11, No. 2 pp. 55-81, 2002.

Comparisons of Various Spinodal Decompositions Theories to Small Angle Light Scattering Experiments of Tetramethyl-Bisphenol-A-Polycarbonate and Polystyrene

M.L.Supakanok THONGYAI, Sirirat WACHARAWICHANANT, and Tharathon MONGKHONSI

Petrochemical Engineering Laboratory, Department of Chemical Engineering,

Faculty of Engineering, Chulalongkorn University

Abstract

This research is concerned with the comparison of the kinetics theories of the autonomous phase separation of polymer blends at high temperatures (Spinodal Decomposition, SD). A set of light scattering data which consisted of intensity, angle and time was used. The blends of Tetramethyl-Bisphenol-A-Polycarbonate (TMPC) / Polystyrene (PS) at 30%, 50% and 70%w of TMPC at various temperatures were examined by small angle light scattering. These light scattering data were examined and compared with predicted values from various theories.

There are four famous kinetics theories, which have the data to support the precision of the predictions that are used in this study. The well-known theory of Cahn and Hilliard (1971) has been used. Further more, the Langer, *et al.* (1975) theory and the theory of Nauman and Balsara (1989) which were both modified from the Cahn and Hilliard (1971) theory, were also investigated. The new theory from Akcasu, *et al.* (1992) was also fitted with the data. The experimental data was fitted with these four theories and compared with the percent relative average error that deviated from the data. The percent relative average error from each equation was tested and analyzed.

The observations of the error proved that the new theory of Akcasu, *et al.* (1992) was the most versatile theory which can be fitted with the two sets of data. The Langer, *et al.* (1975) fitted results show the flexibility of the usage of the theory but the values from the theory can not be related to the basic properties of the phase separated of polymer blend as Akcasu, *et al.* (1992) theory can. The theories that were invented by Nauman, *et al.* (1994); and Cahn, *et al.* (1971) can be well fitted only in the beginning of the spinodal decomposition process. However, we can hardly conclude the validity of the theories based on a consideration of a small amount of data.

Introduction

The dynamics of the spinodal decomposition phenomenon has been investigated both theoretically and experimentally in the field of small molecules concerning binary alloys, fluid mixtures, and inorganic glasses. In recent years, such studies have also become popular in the field of polymer blend systems. The process of spinodal decompositions occurring in polymer blends can be qualitatively classified into three time regimes: (i) the early stage, where the spatial concentration fluctuations increase in amplitude while preserving the same wavelength; (ii) the intermediate stage, where both the amplitude and the wavelength increase with time; and (iii) the late stage, where the amplitude reaches the equilibrium value and only the wavelength grows with time (Cahn, *et al.* 1971; Gennes, 1980; and Binder, 1983).

For the early stage, the validity of the linear Cahn and Hilliard (1971) theory (Cahn, 1971; and Cahn, *et al.* 1971) has been examined with many experimental studies for polymer blends. However, the theory does not account for the intrinsically nonlinear effects in the later stages. In the intermediate stage the nonlinear effects that are ignored in the Cahn and Hilliard (1971) theory are known to become important, and the time dependency of the characteristic quantities exhibits a different behavior than in the early and late stages. These theories have attempted to incorporate nonlinear effects into a theory of spinodal decomposition. Langer, *et al.* (1975) have presented successful theories to date. Other theories, that studied spinodal decomposition are the Akcasu, *et al.* (1992) theory Akcasu, *et al.* (1992) and Nauman, *et al.* 1989; and Nauman, *et al.* 1994 theory. These theories were created to explain the experimental results and modified the Cahn and Hilliard (1971); and Langer, *et al.* (1975) theories.

There were many research who observed the spinodal decomposition of polymer blends, but little research was done to study the theory of spinodal decomposition to explain the experimental results with a new method. For example, the spinodal decomposition of polymer blends was studied by Wang, Z.Y., *et al.* (1993). They studied the nonlinear theory of Langer, *et al.* (1975) with a new calculation method. They found that the results compared well with the experimental data for a polymer-blends system with respect to the value of theory. It was shown that the Langer, *et al.* (1975) theory can be used to describe the phase-separation behavior up to intermediate stages.

In this study, various theories of spinodal decomposition were studied. By fitting each theory with the same experimental data sets, the validity of the theories can be tested. The theories

of Cahn and Hilliard (1971); Langer, *et al.* (1975); Akcasu, *et al.* (1992); and Nauman, *et al.* (1989) were chosen in this study, and nobody has investigated these theories using the same data sets. Therefore, the study of spinodal decomposition with new techniques is very interesting. The study of each theory is very difficult because some theories are not in the form of structure function or intensity function, and we therefore have to change them into an appropriate form and then use them to fit data and calculate the intensity data of the spinodal decomposition theory.

From the application of various spinodal decomposition theories, we will calculate the derivation of experimental data from each theory, and then we will analyze it to find the best theory that can be explained with the experimental results. Moreover, we will analyze the difference between the experimental data and the predicted value from each theory.

Experiments

Materials

The blends selected for these experiments were tetramethyl-bisphenol-A-polycarbonate (TMPC) and polystyrene(PS). TMPC was kindly supplied by BASE, Germany. PS was an industrial grade polystyrene. This blend was selected because of its high glass transition temperature, its good mechanical properties, and for its appearance in a wide range of previous studies. The high glass transition temperature will allow the sample to be quenched and consequently freeze the high temperature morphologies at room temperature. The good mechanical properties provide a wide range of tests which can be made on thin film samples.

Sample preparation

Three blend compositions (30, 50, 70%w) were prepared by solvent casting in toluene. The samples were prepared by casting the solution onto 16 mm glass cover slips and kept at room temperature until they became solid. It was further dried in a vacuum oven at 80°C for 4 days and at 140°C for 7 days.

Light Scattering techniques

Experimental results were performed using light scattering apparatus. The equipment is schematically shown in Figure 1. An aerotech model 1105P He/Ne laser of 5 mW (λ=632.8 nm) is used as a light source incident on a sample inside a temperature controlled sample holder. The scattered light was detected by a photo diode array, mounted on an arc between 5-67 degrees at 2-degree intervals. The signal is then converted in a multi-channel analogue/digital converter. Control and data collections are both implemented using a PC.

The wave vector, q can be expressed as a function of the wave length of the laser, λ and the scattered angle, θ;

$$q = \frac{4n\pi}{\lambda}\sin\left(\frac{\theta}{2}\right) \qquad (1)$$

The light scattering instrument is the instrument that can indirectly measure the concentration fluctuations of a polymer blend. It measures the scattered light intensity at various angles and times that results from the changes in the refractive indices of the sample. When phase separation occurs, the two different phases induce a difference in refractive index that results from an increase in the concentration fluctuations of the polymer blend.

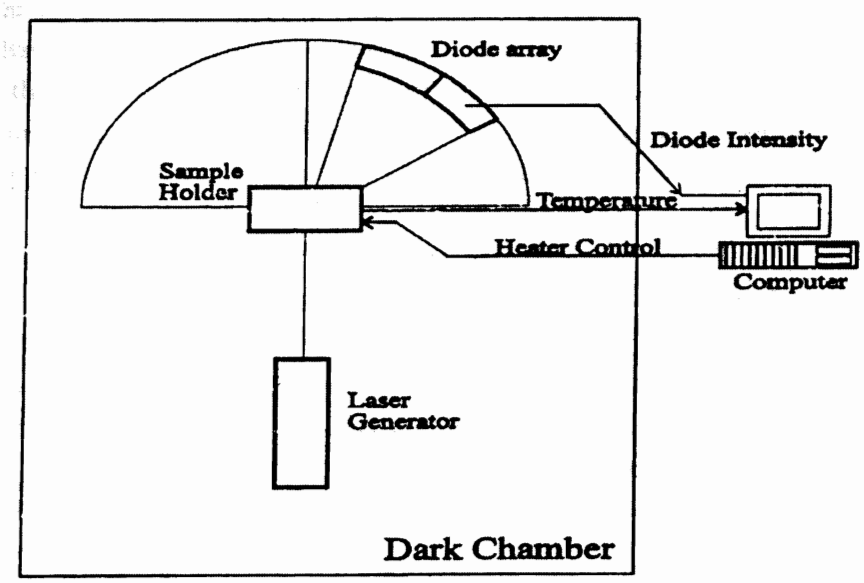

Figure 1 Small Angle Light Scattering Machine Thongyai, (1994)

Two different methods were employed using the light scattering apparatus, viz. cloud point experiments, and a temperature jump experiment. In the former case, a number of dry films of each composition were heated at different heating rates. The point at which the scattered intensities start to increase is defined as the cloud point as shown in Figure 2. This is because cloud point values depend on the rate at which phase separation in the sample responds to the temperature changes. Three heating rate experiments (0.8,0.4,0.1°C/min) for each of the compositions (30, 50, 70%w TMPC) were chosen. The zero heating rate cloud points were obtained by extrapolation from the three heating rate temperatures to the zero heating rate temperature. The cloud point of the three compositions were obtained by this method. The extrapolations are show in Figure 3.

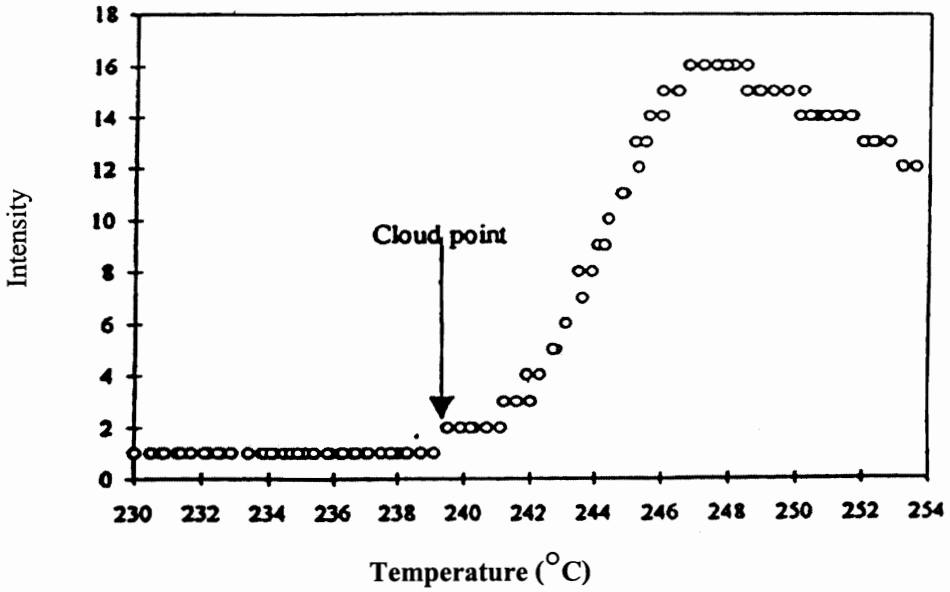

Figure 2 A plot of Intensity against temperature.

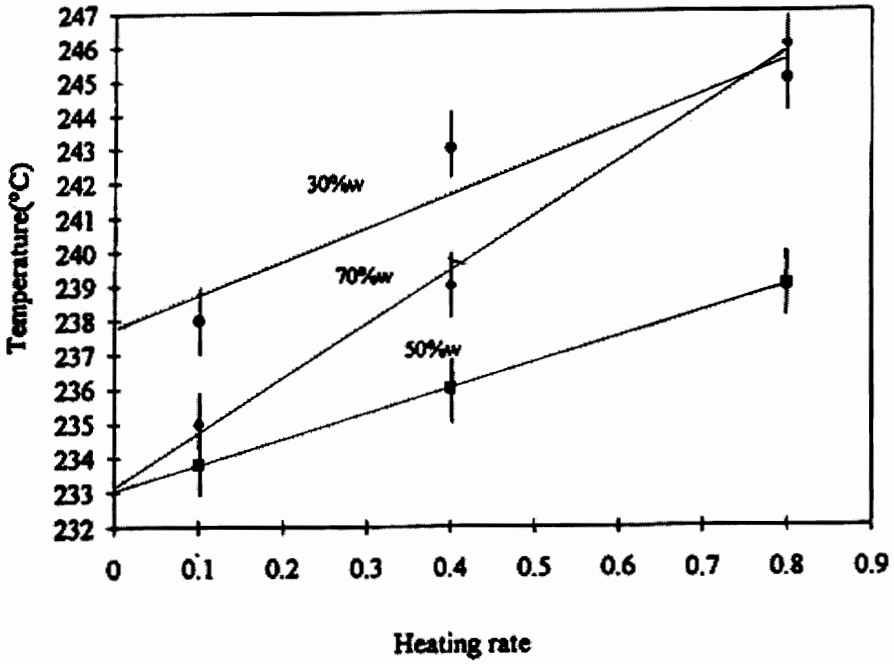

Figure 3 Linearised curve fitting.

The second set of experiments was designed to determine the spinodal temperatures, by following the spinodal decomposition process after a temperature jump inside the phase boundary. To obtain the temperature jump experiment, the cover slip samples were annealed at 200±5°C for 5 minutes and then transferred quickly into the sample holder, which was preheated to the desired temperature inside the phase boundary. The He-Ne laser was projected through the sample while N_2 was blowing continuously to cover the sample in order to prevent the degradation of the sample. The rate of change of intensity with time on each of the photodiodes provides the Cahn and Hilliard (1971) growth rate (R(q)). The intensity and time curve can be fitted by taking natural logarithm intensity (ln I) and fitting it with a straight line. The R(q) are obtained from half of the slope of the fitted line as seen in Figure 4.

The growth rate (R(q) leads to a definition of the apparent diffusion coefficient, $D_{app} = [R(q)/q^2]_{q->0}$. In other words, The D_{app} can be obtained from the intercept of a plot of $R(q)/q^2$ versus q^2 as shown in Figure 5. Spinodal points therefore can be obtained by extrapolating the apparent diffusion coefficient to zero as shown in Figure 6.

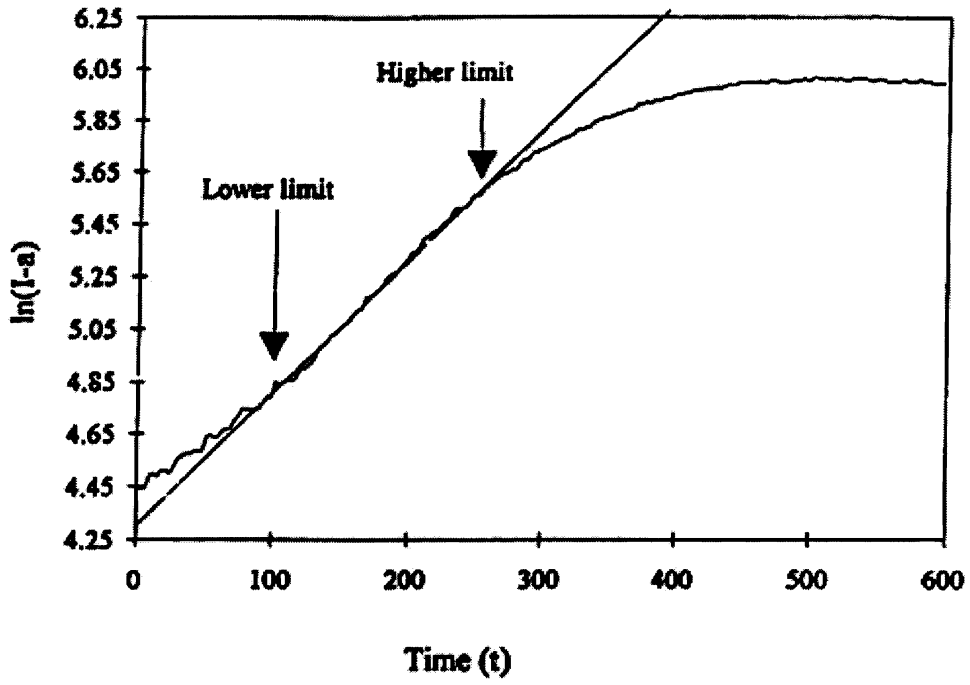

Figure 4 A plot of temperature against heating rate for 30,50,70%w TMPC.

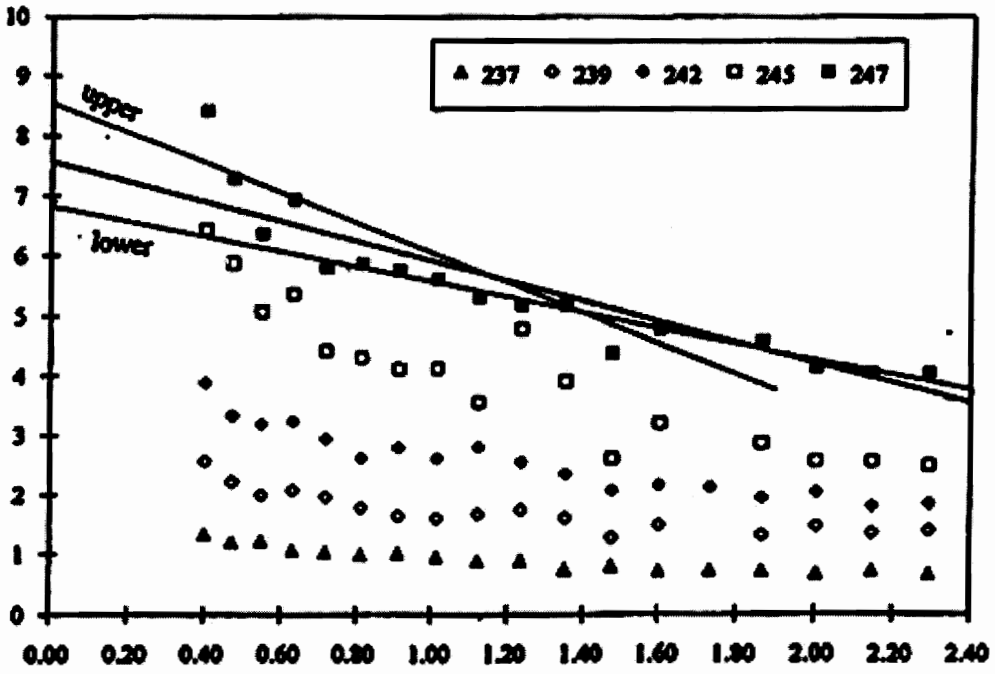

Figure 5 A plot of $R(q)/q^2$ against q^2 of 50 %w TMPC at five temperatures.

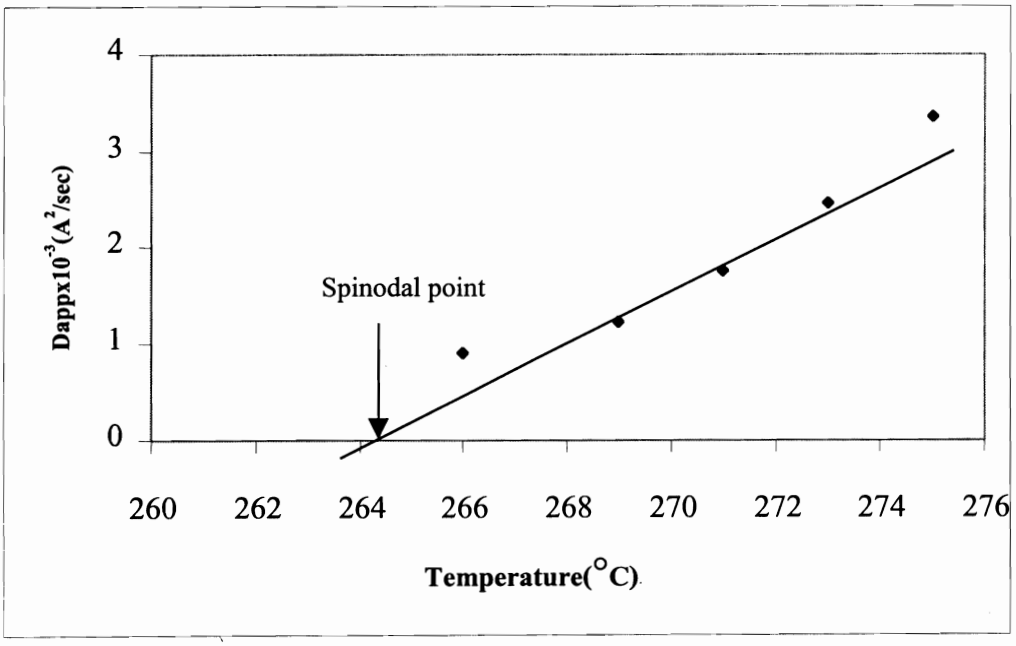

Figure 6 A plot of D_{app} against temperature of 30 %w TMPC at five temperatures and the spinodal temperature can be obtained from extrapolating D_{app} to zero.

Analysis of Experimental Data

The experimental results that are used to fit data were obtained from the temperature jump experiment. The data are the intensities at various angles and various times of the sample at the specific temperature. The experimental results used in this study are the ones of the system of tetramethyl-bisphenol-A-polycarbonate (TMPC)/polystyrene (PS) blends at five temperature jumps. Three compositions (30, 50, 70%w TMPC/PS blends) of this blend were prepared by solvent casting. This set of experimental results was obtained from the study of Thongyai (1990); and Thongyai (1994).

1. Analysis of the Cahn and Hilliard (1971) Theory

According to the Cahn and Hilliard (1971) theory, the intensity can be calculated from equation

$$S(q,t) = S_x(q) + (S(q,o) - S_x(q))\exp(2R(q)t) \qquad (1)$$

The data are the intensities at various angles and times of the sample at a specific temperature. The intensity-time curve can be fitted by taking the natural logarithm of Intensity (In I) and fitting it with a straight line. The data obtained is the growth rate .The $R(q)$ values are obtained from half of the slope of the fitted line.

Where the term of thermal noise that is very small and often negligible, and $S[q,o] - S_x(q)$ is the intensity factor, we use the equation (1.1) to calculate the intensity data of the Cahn and Hilliard (1971) theory at constant q and different times. Then, we compare the calculated intensity data with the experimental data received from Thongyai (1994).

2 Analysis of Langer, *et al.* (1975) Theory

From Langer, *et al.* (1975) theory, we will use equation (2.2) to find the intensity data.

$$\frac{\partial S(q,t)}{\partial t} = -2Mq^2\left[Kq^2 + A(t)\right]S(q,t) \qquad (2.2)$$

This equation is more complicated than the normal Cahn and Hilliard (1971) equation.

The term *A(t)* in equation (2.2) can be solved by using the power law, which can be expanded as,

$$A(t) = a + bt + ct^2 + dt^3 \qquad (2.3)$$

When we substitute equation (2.3) into equation (2.2), we will obtain

$$\frac{1}{S(q,t)}\partial S(q,t) = -2Mq^2\left[Kq^2 + a + bt + ct^2 + dt^3\right]\partial t \qquad (2.4)$$

Then, we can solve this equation by integrating both sides of the equation as,

$$\ln(S(q,t)) - \ln(S(q,o)) = -2Mq^2\left[Kq^2t + \frac{a}{1}t + \frac{b}{2}t^2 + \frac{c}{3}t^3 + \frac{d}{4}t^4\right] \qquad (2.5)$$

$$\ln(S(q,t)) = -2MKq^4t + q^2\left(a't + b't^2 + c't^3 + d't^4\right) + E \qquad (2.6)$$

When q is given as a constant, we can write equation (2.6) in a simple form as follows:

$$\ln(S(q,t))_q = (E + At + Bt^2 + Ct^3 + Dt^4)_q \quad (2.7)$$

Where A, B, C and E are the total coefficients of any q at different time, values and E is the intensity factor. Equation (2.7) is the basic equation that can be used to fit experimental data at constant q and different time values by using the MATHEMATICA program. From the fit data, we get the total coefficients and the intensity factor. Then, we substitute these values into equation (2.7) at different time values to calculate the new intensity data of Langer, *et al.* (1975) theory. Finally, we compare results between the intensity data from calculation and the experimental data.

Langer, *et al.* (1975) theory differs from the other theories by factor $A(t)$ that was expanded using the power law to simplify equation (2.7) for calculations. The intensities were calculated using only exponents from the fitted equation.

3. Analysis of Akcasu, *et al.* (1992) Theory

We obtain the equation of Akcasu, *et al.* (1992) theory from equation (3.1), which can then be used to calculate the intensity $I(q,t)$.

$$\frac{dI(q,t)}{dt} = -2R(q)I(q,t)[1 + Z(q,t)] + C(q) \quad (3.1)$$

From equation (3.1), when q is constant then the term of $Z(q,t)$ can be expanded using the power law as follows:

$$Z(q,t)_q = A' + B't + C't^2 + D't^3 \quad (3.2)$$

After we substitute for equation (3.2) in equation (3.1), we will obtain the intensity equation as

$$\frac{dI(q,t)}{dt} = -2R(q)I(q,t)[1 + A' + B't + C't^2 + D't^3]_q + C(q) \quad (3.3)$$

C(q) is very small and often negligible, therefore we can integrate equation (3.3) numerically using the Explicit Euler's law as follows:

$$\left(\frac{I(q,t+\Delta t) - I(q,t)}{\Delta t}\right)_q = -2R(q)I(q,t)[A'' + B't + C't^2 + D't^3]_q \quad (3.4)$$

When $A'' = 1 + A'$ and A'', B', C', D' are coefficients of equation, is there an equation number missing? we must rearrange equation (3.4) to calculate intensity, and it can be written as follows:

$$I(q,t+\Delta t)_q = I(q,t)_q - 2R(q)I(q,t)\Delta t[A' + B't + C't^2 + D't^3]_q \quad (3.5)$$

After we calculate intensity from equation (3.5), we use these calculated results to compare with the experiment results.

4. Analysis of Nauman and Balsara (1989) Theory

The equation of Nauman and Balsara (1989) theory can be written as follows:

$$\frac{\partial a(x,t)}{\partial t} = D_{AB}\nabla a(x,t)(1 - a(x,t))[g''\nabla a(x,t) - \kappa\nabla^3 a(x,t)] \quad (4.1)$$

Here $a(x,t)$ is a mole fraction. For the sake of simplicity, considering one dimension of x, one can obtain

$$\frac{\partial a(x,t)}{\partial t} = D_{AB}\frac{\partial}{\partial x}a(x,t)(1-a(x,t))\begin{bmatrix} g''\dfrac{\partial}{\partial x}a(x,t) \\ -\kappa\dfrac{\partial^3}{\partial x^3}a(x,t)\end{bmatrix} \quad (4.2)$$

This equation can be modified by Fourier transformation to relate it with the structure function, and substitution of $\partial/\partial x$ by iq. The Fourier transform of equation (4.2) can be written as,

$$\frac{\partial a(q,t)}{\partial t} = D_{AB}(iq)a(q,t)(1-a(q,t))\begin{bmatrix} g''(iq)a(q,t)- \\ \kappa(iq)^3 a(q,t)\end{bmatrix} \quad (4.3)$$

Equation (4.3) then can be modified.

$$\frac{\partial a(q,t)}{\partial t} = D_{AB}a(q,t)(1-a(q,t))\begin{bmatrix} -(g''q^2 a(q,t))- \\ (\kappa q^4 a(q,t))\end{bmatrix} \quad (4.4)$$

$$\frac{\partial a(q,t)}{\partial t} = D_{AB}(-g''q^2-\kappa q^4)(a^2(q,t)-a^3(q,t)) \quad (4.5)$$

We have the definition of the structure function $(S(q,t))$ below,

$$S(q,t) = \langle |a(q,t)|^2 \rangle = \langle a(q,t).a(-q,t) \rangle \quad (4.6)$$

Differentiating the structure function as below:

$$\frac{\partial S(q,t)}{\partial t} = a(-q,t).\frac{\partial a(q,t)}{\partial t} + a(q,t).\frac{\partial a(-q,t)}{\partial t} \quad (4.7)$$

From equation (4.5) and (4.7), the structure function can also be written as follows:

$$\frac{\partial S(q,t)}{\partial t} = \begin{Bmatrix} a(-q,t)D_{AB}(-g''q^2-\kappa q^4)(a^2(q,t)-a^3(q,t))+ \\ +a(q,t)D_{AB}(-g''q^2-\kappa q^4)(a^2(q,t)-a^3(q,t))\end{Bmatrix} \quad (4.8)$$

It should be noted that a does not depend on the sign of q, or $da(q,t)/dt$ is equal to $da(-q,t)/dt$, so equation (4.8) can be written as below.

$$\frac{\partial S(q,t)}{\partial t} = \begin{Bmatrix} D_{AB}(-g''q^2-\kappa q^4)(a^3(q,t)-a^4(q,t)) \\ +D_{AB}(-g''q^2-\kappa q^4)(a^3(q,t)-a^4(q,t))\end{Bmatrix} \quad (4.9)$$

We will obtain the structure equation as in equation (4.10).

$$\frac{\partial S(q,t)}{\partial t} = 2D_{AB}(-g''q^2-\kappa q^4)[S(q,t).a(q,t)-S^2(q,t)] \quad (4.10)$$

From equation (4.10), it can be written as follows:

$$\frac{1}{[S(q,t).a(q,t)-S^2(q,t)]}\frac{\partial S(q,t)}{\partial t} = 2D_{AB}(-g''q^2-\kappa q^4) \quad (4.11)$$

It is assumed that the a value is the mole fraction and it is very small (a < 1) so it can be neglected when compared with the structure function. Then, we can write the equation as,

$$\frac{1}{-S^2(q,t)}\frac{\partial S(q,t)}{\partial t} = 2D_{AB}(-g''q^2-\kappa q^4) \quad (4.12)$$

Because the structure function is directly proportional to the intensity, we can calculate the intensity $I(q,t)$ and equation (4.12) can be rewritten as,

$$\frac{1}{-I^2(q,t)}\frac{dI(q,t)}{dt} = 2D_{AB}\left(-g^{''}q^2 - \kappa q^4\right) \quad (4.13)$$

From equation (4.13), when t is constant but q is varied, we can arrange this equation to fit the data as follows:

$$\frac{1}{-I^2(q,t)}\frac{dI(q,t)}{dt} = \left(A'''q^2 + B''q^4\right) \quad (4.14)$$

Where A''', B'' are the coefficients of time constant at different q. We can integrate equation (4.14) numerically using the Explicit Euler principle as follows:

$$\frac{I(q+\Delta q,t) - I(q,t)}{-I^2(q,t)\Delta t} = \left(A'''q^2 + B''q^4\right) \quad (4.15)$$

We use the experimental results to find the coefficients A''', B''. In order to calculate the intensity at constant q and different time, we shall insert those coefficients in to equation (4.15). So, we can rewrite equation (4.15) in the following form:

$$\frac{I(q,t+\Delta t) - I(q,t)}{-I^2(q,t)\Delta t} = \left(A'''q^2 + B''q^4\right) \quad (4.16)$$

$$I(q,t+\Delta t) = I(q,t) - I^2(q,t)\Delta t\left(A'''q^2 + B''q^4\right) \quad (4.17)$$

The coefficients parameters A''', B'', were expanded using the power law as follows:

$$A''' = f + ht + jt^2 + lt^3 \quad (4.18)$$

$$B'' = f' + h't + j't^2 + l't^3 \quad (4.19)$$

It was made in order to consider the A''', B'' parameters as a function of time. These coefficients at one angle were fitted with equation (4.18) and (4.19) using the MATHEMATICA program. From the fit data, we obtain the coefficients parameter; blends at

$$I(q,t+\Delta t)_q = I(q,t)_q - I^2(q,t)\Delta t\left[\begin{matrix}\left(f + ht + jt^2 + lt^3\right)q^2 \\ + \left(f' + h't + j't^2 + l't^3\right)q^4\end{matrix}\right] \quad (4.20)$$

From equation (4.20), the intensity data of Nauman and Balsara (1989) theory can be calculated by substituting the coefficients. Then, we compare the calculated intensity with the experimental data.

Nauman and Balsara (1989) theory differs from the Cahn and Hilliard (1971) theory by a factor of $a(1-a)$ and differs from that of the other theories in the way that they are treated in structure function $(S(q,t))$ and in the details of calculations arising from equation (4.5). Equation (4.5) was used to calculate the simulation data. Inserting time step (Δt) and intensity values from the experiment into equation (4.6) can provide a coefficient parameter using the MATHEMATICA program, after these coefficient parameters were expanded using the power law. These coefficient parameters fitted with equation (4.2.9) and (4.2.10) can provide new coefficient parameters; f, h, j, l, f', h', j' and l'.

5. Summary

So far, various theoretical approaches regarding the kinetics of phase separation via spinodal decomposition of a binary system have

been analysed. The first and most well-known theory is the Cahn and Hilliard (1971) theory. The second theory is the Langer, *et al.* (1975) theory, which differs from the other theories by a factor of A(t). The A(t) factor is the Fourier transformation of the higher-order correlation function. The third theory is the Akacu, *et al.* (1992) theory. This theory approach is essentially the same as the one developed by Langer, *et al.* (1975). This is included in the nonlinear theory, and in the details of the calculations arising from the chain connectivity (polymer effect) in the case of polymer blends. In addition, the variation of the scattering wave numbers is studied not only during spinodal decomposition but also during dissolution. Akcasu, *et al.* (1992) theory differs from the other theories by factor Z(q,t), which is the polymer effect term. The last theory is Nauman and Balsara (1989) theory. Nauman and Balsara (1989) theory differs from the Cahn and Hilliard (1971) theory by factor of a(1-a) and differs from that of the other theories in the way that it is treated in structure function(S(q,t)) and the details of the calculation.

Results & Discussions

Part I. Results of Intensity Calculated from each Theory

The angle for scattered light intensity at 35° was the angle at which the spinodal peaks were observed for the 30%w and 70%w TMPC/PS blends. So, we consider intensities at this angle.

Figure 7 shows the intensity data calculated from various theories of 30%w TMPC/PS blends at $271^{\circ}C$ and at the angle of 35°, it appeared that the intensity of Cahn and Hilliard (1971) theory smoothly increases with increasing time. The intensities of Akcasu, *et al.* (1992); and Langer, *et al.* (1975) are quite similar to the intensity found from the experiment. The results of Nauman, *et al.* (1994); and Cahn, *et al.* (1971) greatly differ from experimental results. It shows that the Akcasu, *et al.* (1992); and Langer, *et al.* (1975) theories can be used to fit the data better than the other two theories.

Figure 8 shows the intensity calculated from various theories of 50%w TMPC/PS blends at $239^{\circ}C$ and at the angle of 35°, it appeared that the intensity of the Cahn and Hilliard (1971) theory smoothly increases with increasing time. The intensities of Akcasu, *et al.* (1992); and Langer, *et al.* (1975) are quite the same as the experimental ones. At the beginning of the spinodal decomposition process, the results of Cahn and Hilliard (1971) theory do not differ from experimental results, but at longer times the differences are larger. It shows that the Cahn and Hilliard (1971) theory can be explained only at the beginning of phase decomposition. The intensities

of Akcasu, *et al.* (1992) and Langer, *et al.* (1975) theories can be used to fit the data better than the other two theories. So these two theories can be used to explain this system at all ranges of testing. In Figure 7, the intensities predicted by Nauman and Balsara (1989) have small errors.

Figure 9 shows the intensity calculated from various theories of 70%w TMPC/PS blends at 297°C and at an angle of 35°. It appears that the intensity of Cahn and Hilliard (1971) theory smoothly increases with increasing time. For this system, the intensity from Akcasu, *et al.* (1992) theory seems to give the best fit to the experimental data compared with other theories.

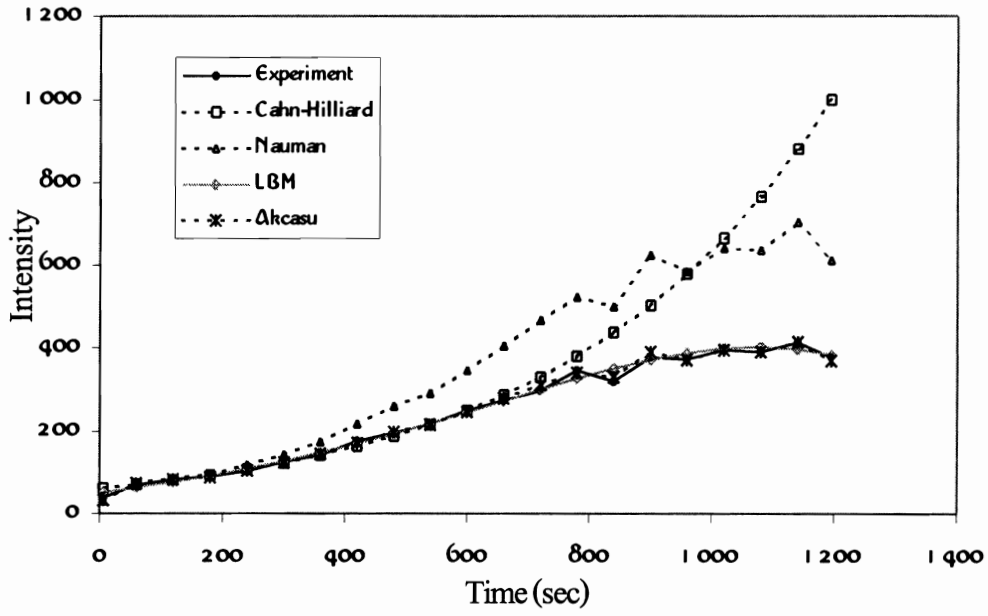

Figure 7 The intensity data of 30%w TMPC/PS blends at 271°C and the angle of 35°, obtained from the experiment and calculated from various theories.

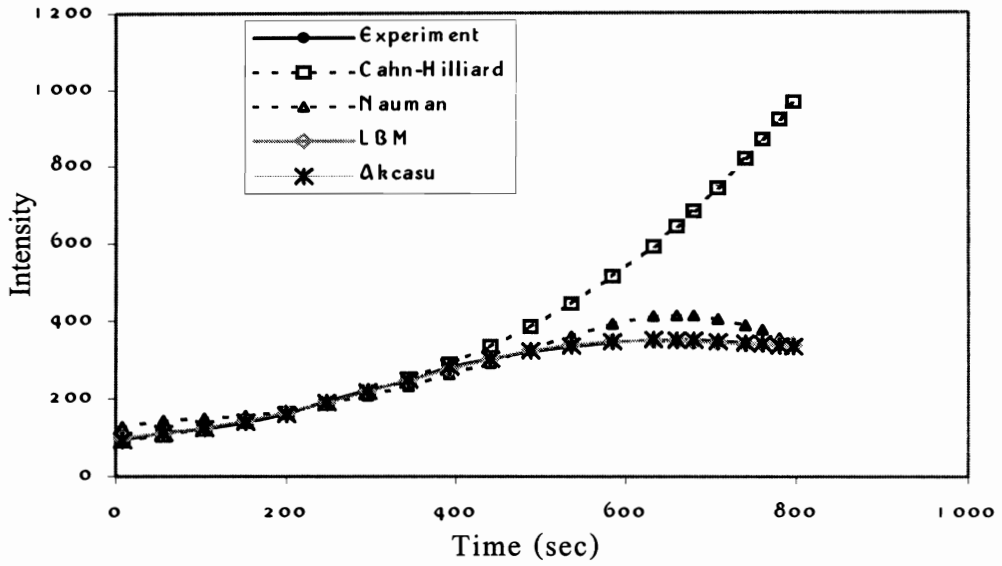

Figure 8 The intensity data of 50%w TMPC/PS blends at 239°C and the angle of 35°, obtained from the experiment and calculated from various theories.

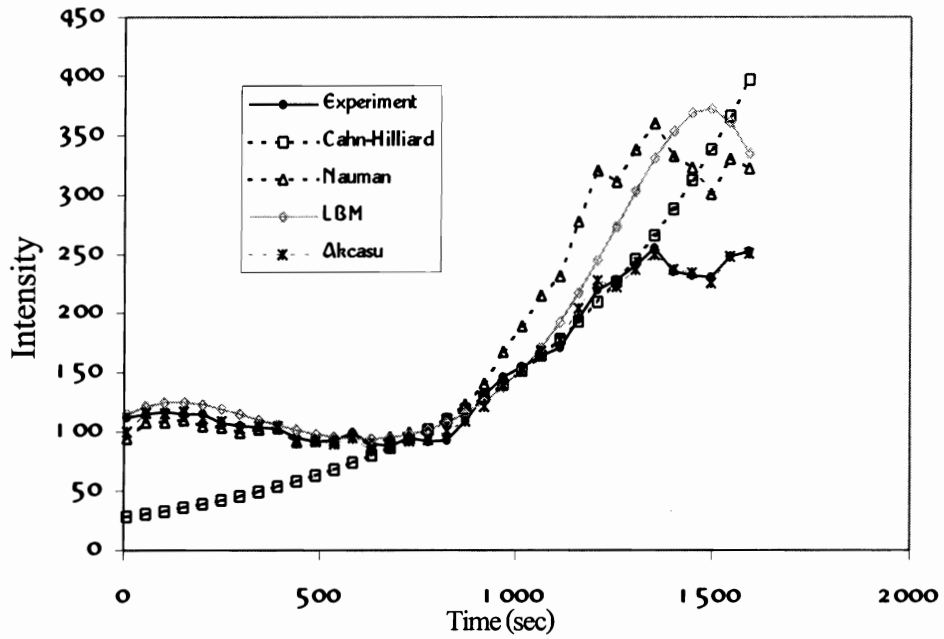

Figure 9 The intensity data of 70%w TMPC/PS blends at 297°C and the angle of 35°, obtained from the experiment and calculated from various theories.

Part II. The Percent Relative Average Error Results of TMPC/PS Blends

The percent relative average error is calculated by

% Relative Average Error =

$$\frac{\sum_{t=1}^{n}\left|\frac{I_{Exp,t}-I_{Th,t}}{I_{Exp,t}}\right|(100)}{n}$$

Where I_{Exp} = Experimental data

I_{Th} = Calculated data of each theory

n = Number of data

t = time

The Percent Relative Average Error Results of 30%w TMPC/PS Blends

In Figure 10, it shows the percent relative average error between experimental and calculated results from Cahn and Hilliard (1971) theory at any angle. When the angle scattering increased, the percent relative average error increased at all five temperatures. From graph patterns, they show that the different temperatures, the different intensities that predicted from the theories and minus by the real data difference from each other too. Low temperatures have a less percent relative average error than the higher temperatures. In Figure 11 and Figure 12, they show the percent relative average error of Langer, *et al.* (1975); and Akcasu, *et al.* (1992) theories respectively. When the angle scattering increased, most of the percent relative average errors did not vary at the five different temperatures. At 266°C, 269°C and 271°C Akcasu, *et al.* (1992) theory has a less percent relative average error than at the higher temperatures (273°C and 275°C). These results show that temperature will to influence the testing fit data of testing, and at low temperatures it is possible to fit the experimental results better than at higher temperatures. From the fitted experimental data of Nauman and Balsara (1989) theory, it is show that the high temperature data has a less total difference value than the lower temperature data. The intensities differ from the other theory. At 266°C there is a large variation from the experimental result as show in Figure 13. The percent relative average error increased at low angles, and decreased at high angles.

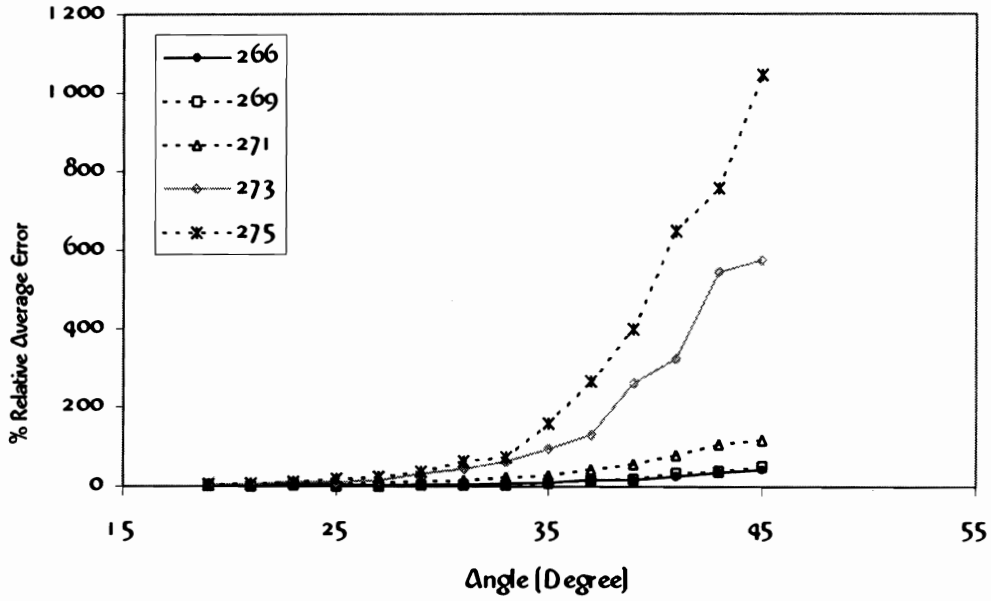

Figure 10 The percent relative average error of 30%w TMPC/PS blends at different temperatures, calculated from Cahn and Hilliard (1971) theory.

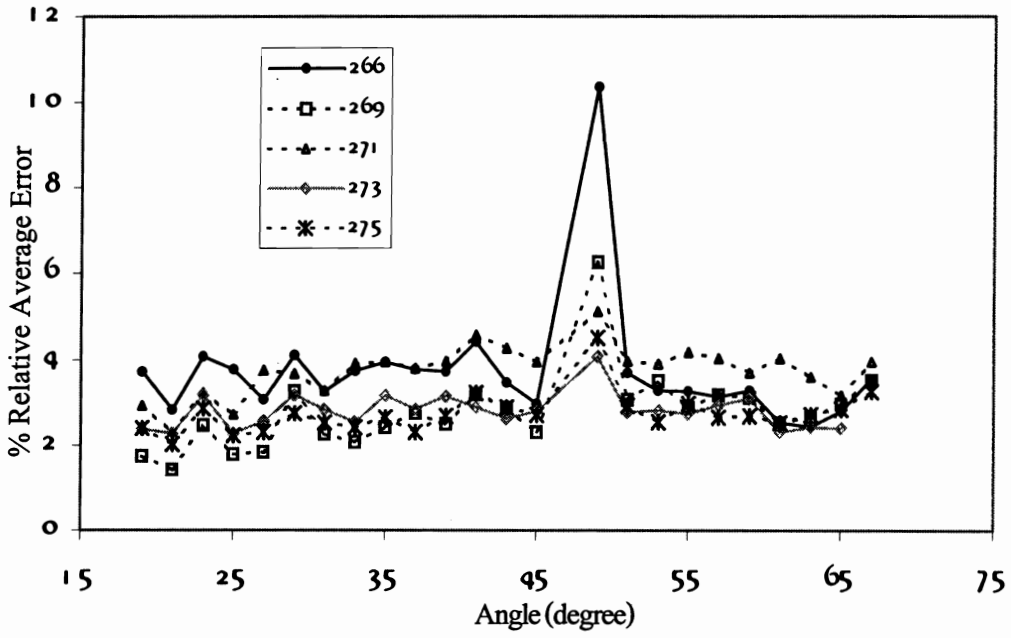

Figure 11 The percent relative average error of 30%w TMPC/PS blends at different temperatures, calculated from Langer, *et al.* (1975) theory.

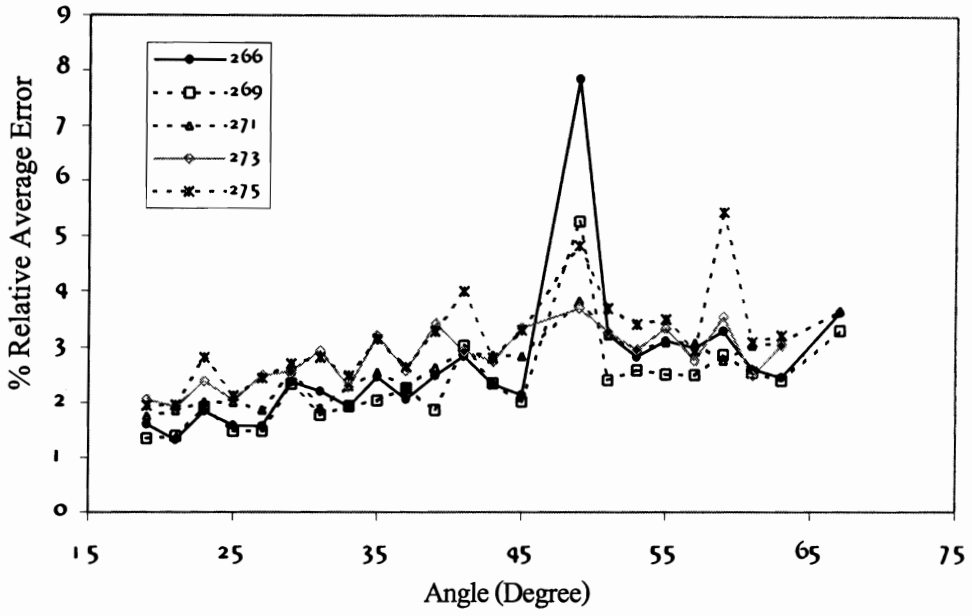

Figure 12 The percent relative average error of 30%w TMPC/PS blends at different temperatures, calculated from Akcasu, *et al.* (1992) theory.

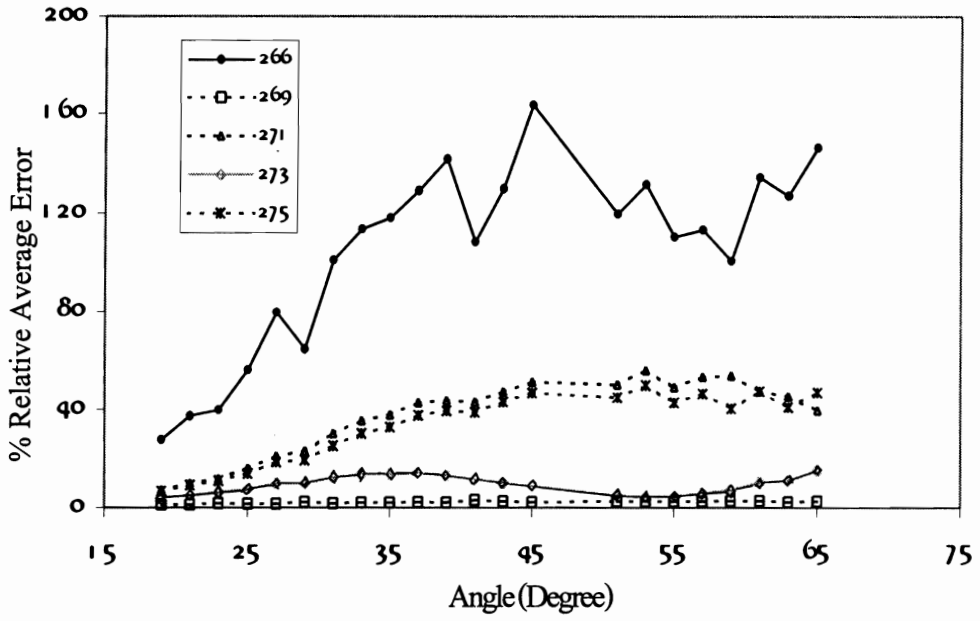

Figure 13 The percent relative average error of 30%w TMPC/PS blends at different temperatures, calculated from Nauman and Balsara (1989) theory.

The Percent Relative Average Error of 50% TMPC/PS Blends Results

In Figure 14, it shows the percent relative average error results of Cahn and Hilliard (1971) theory. When the angle for scattered intensity increased, the percent relative average error values increased for every temperature. From the graph patterns, it seems to be that the higher temperatures induce an increase in the percent relative average error values. At low temperatures, the percent relative average error is less than that of the higher temperature data at every angle. It shows that at low temperatures the Cahn and Hilliard (1971) theory can be used to fit experimental results better than at higher temperatures. At high temperature (247°C), the biggest derivation from experimental results was observed for the case of Cahn and Hilliard (1971) theory. The results of Langer, *et al.* (1975) theory are show in Figure 15. At the temperatures of 237°C, 239°C and 242°C, the percent relative average error does not vary much for all angles. But for the temperatures of 245°C and 247°C, they showed higher error values, especially at high angle range. The percent relative error of Akcasu, *et al.* (1992) theory Figure 16 shows that as the angle increased, the percent relative average error values increased for every temperature. Furthermore, the percent relative average error is indifferent to changing temperature. It shows that the intensity from Akcasu, *et al.* (1992) theory can fit well with experimental results. The percent relative average error of Nauman and Balsara (1989) theory was shown in Figure 17. At 239°C, 242°C and 245°C are smooth while the ones at 237°C and 247°C considerably different. It shows that at 237°C and 247°C the percent relative average error is not in a good agreement with this theory.

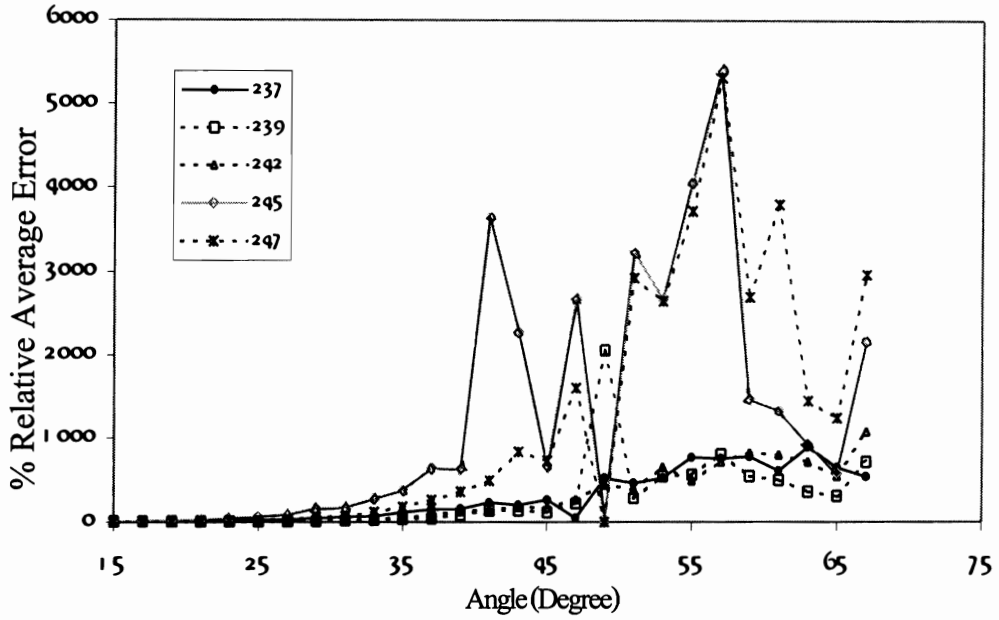

Figure 14 The percent relative average error of 50%w TMPC/PS blends at different temperatures, calculated from Cahn and Hilliard (1971) theory.

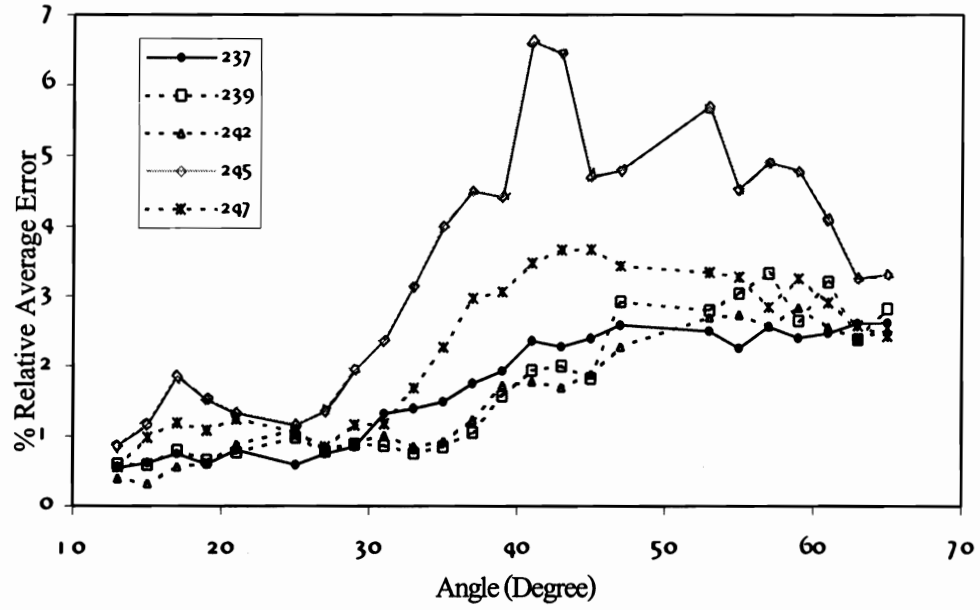

Figure 15 The percent relative average error 50%w TMPC/PS blends at different temperatures, calculated from Langer, *et al.* (1975) theory.

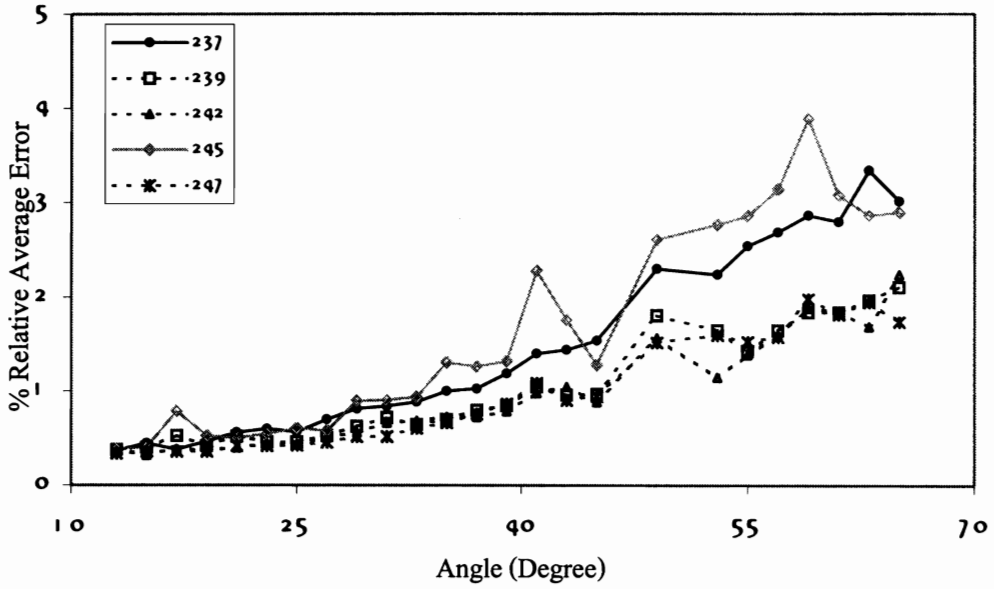

Figure 16 The percent relative average error of 50%w TMPC/PS blends at different temperatures, calculated from Akcasu, *et al.* (1992) theory.

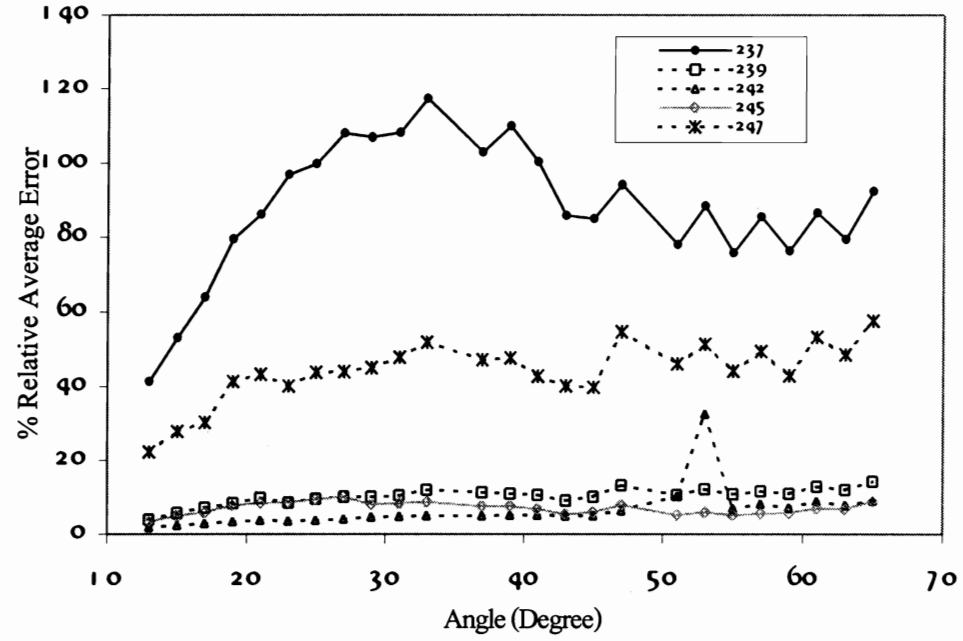

Figure 17 The percent relative average error of 50%w TMPC/PS blends at different temperatures, calculated from Nauman and Balsara (1989) theory.

The Percent Relative Average Error Results of 70%w TMPC/PS Blends

In Figure 18, it shows that for the percent relative average error of Cahn and Hilliard (1971) theory the lower temperatures are where the smaller percent relative average error values are. At 301°C, the experimental data do not well fit by Cahn and Hilliard (1971) theory. It appeared that at higher temperatures the Cahn and Hilliard (1971) theory could not fit well with the experimental data for this system. In Figure 19, it shows that the percent relative average error of Langer, *et al.* (1975) theory slightly changed at different temperatures, it appeared that these results of fitted data are not very different. But at 297°C and low angle values, the percent relative average error is quite high. The percent relative average error of Akcasu, *et al.* (1992) theory is displayed in Figure 20. At 301°C, the experimental data do not fit well by Akcasu, *et al.* (1992) theory. It appeared that at higher temperatures the Akcasu, *et al.* (1992) theory cloud not fit well with the experimental data for this system. Figure 21 displays that the percent relative average error of Nauman and Balsara (1989) theory slightly changes at different temperatures. At 299°C and low angle values, the percent relative average errors are quite high.

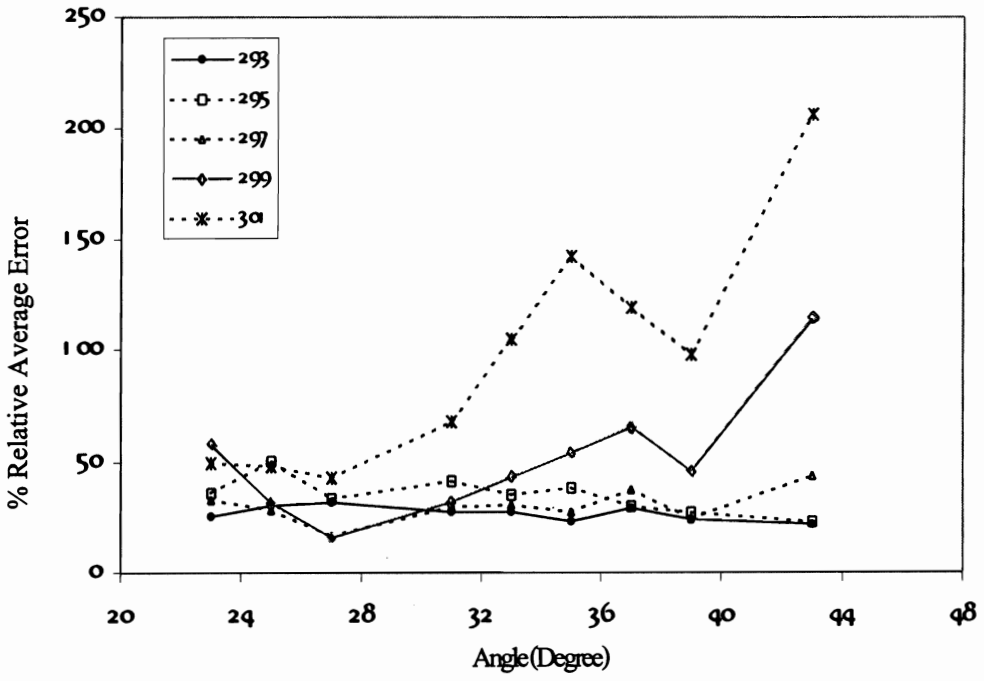

Figure 18 The percent relative average error of 70%w TMPC/PS blends at different temperatures, calculated from Cahn and Hilliard (1971) theory.

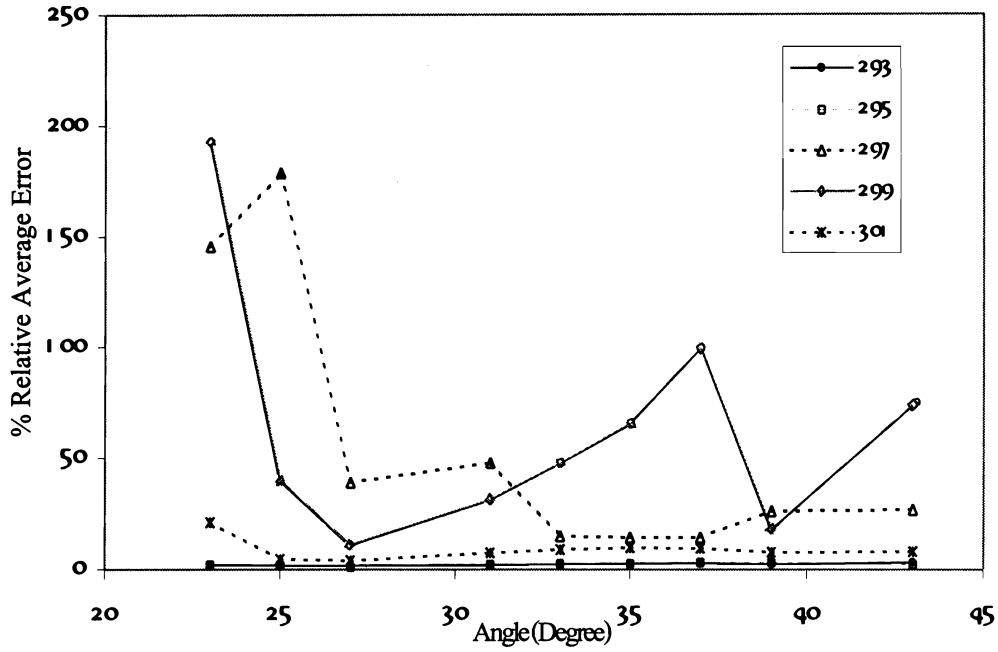

Figure 19 The percent relative average error of 70%w TMPC/PS blends at different temperatures, calculated from Langer, *et al.* (1975) theory.

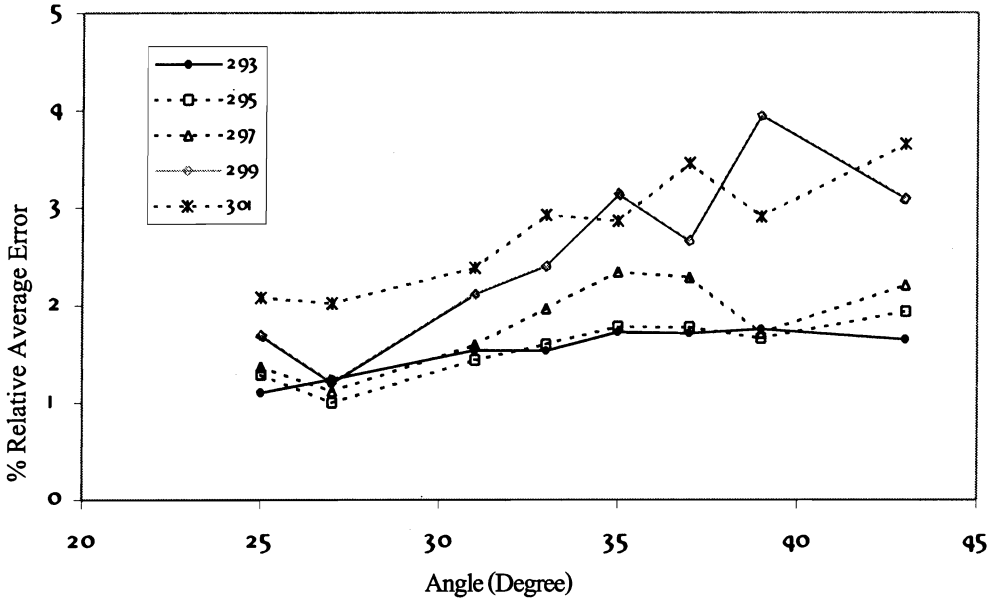

Figure 20 The percent relative average error of 70%w TMPC/PS blends at different temperatures, calculated from Akcasu, *et al.* (1992) theory.

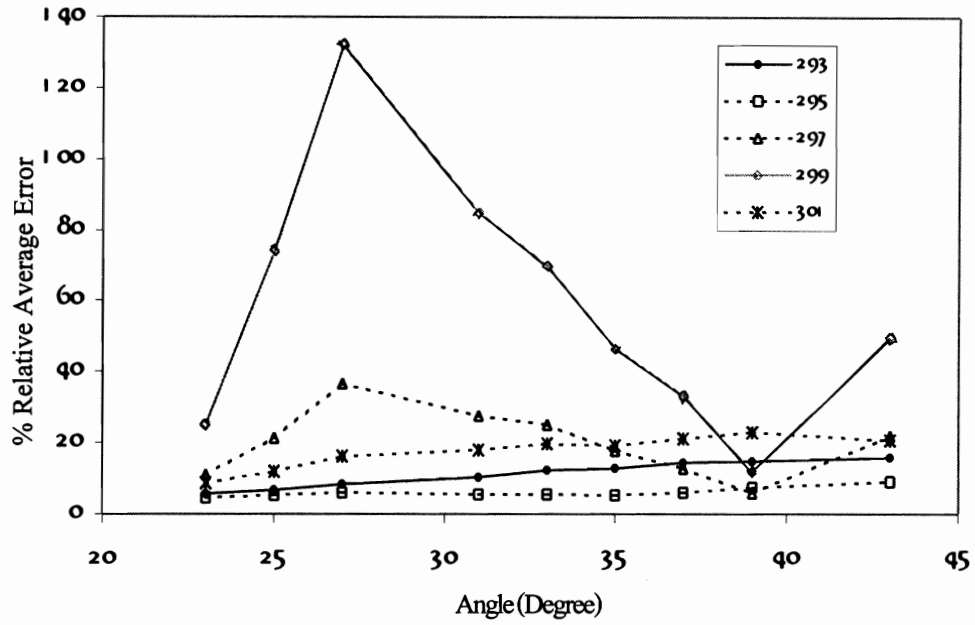

Figure 21 The percent relative average error of 70%w TMPC/PS blends at different temperatures, calculated from Nauman and Balsara (1989) theory.

Part III Comparisons of each Theory

In Figure 22, it shows the percent relative average error of 30%w TMPC/PS blends at the spinodal point of 273°C. The percent relative average errors from Langer, *et al.* (1975); and Akcasu, *et al.* (1992) theories are small. These two theories can fit with experimental data better than the Nauman, *et al.* (1994); and Cahn, *et al.* (1971) theories, and can be used to explain the phase separation data more widely. In Figure 23, it shows the percent relative average error of 50%w TMPC/PS blends at 242°C. It appeared that the percent relative average error from the Langer, *et al.* (1975); and Akcasu, *et al.* (1992) theories are less than those from the Nauman, *et al.* (1994); and Cahn, *et al.* (1971) theories. The percent relative average error of Cahn and Hilliard (1971) theory increases with increasing angles. The percent relative average error of Nauman and Balsara (1989) theory does not change much. Figure 24 displays the percent relative average error of 70%w TMPC/PS blends at 293°C. It appeared that the percent relative average error of each theory is small. The percent relative average errors from the Akcasu, *et al.* (1992); and Langer, *et al.* (1975) theories are not different from each other.

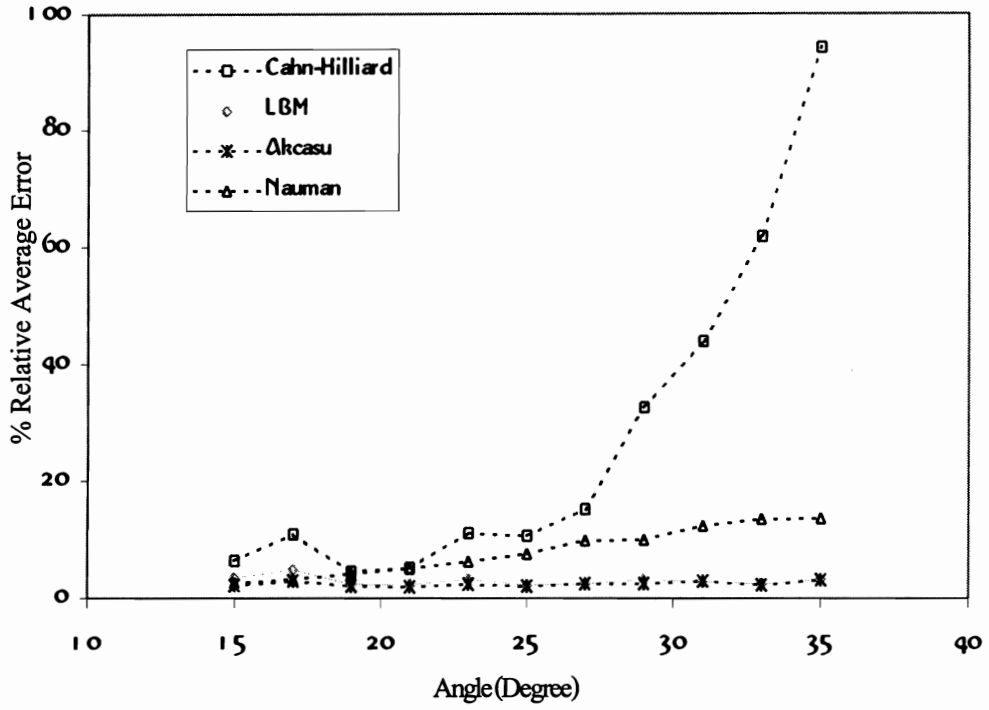

Figure 22 The percent relative average error of 30%w TMPC/PS blends at 273 °C of each theory.

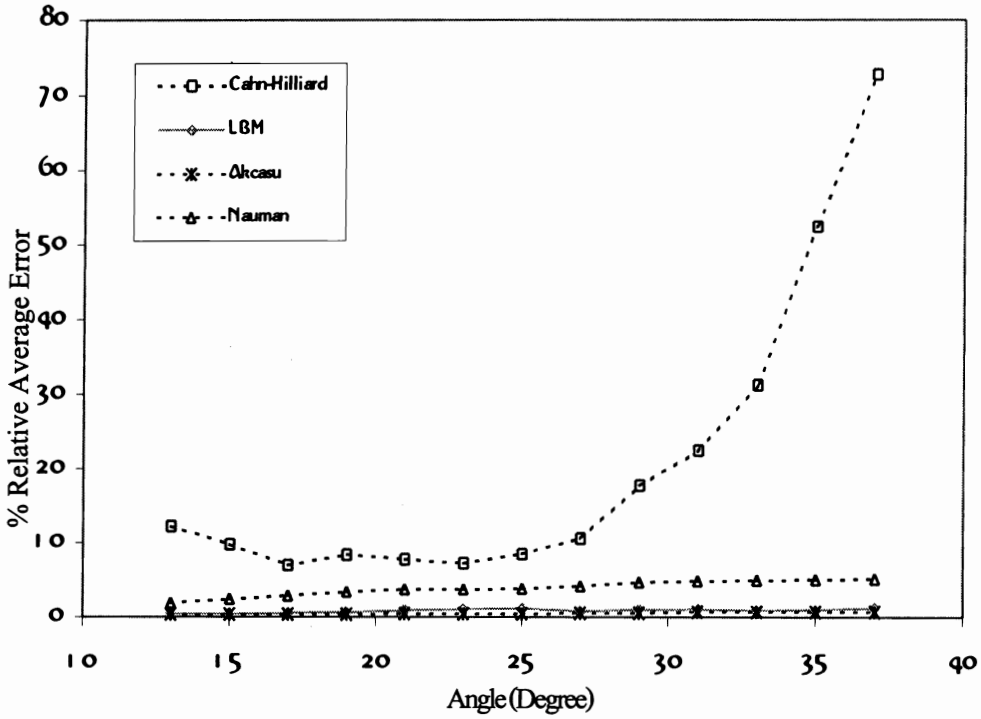

Figure 23 The percent relative average error of 50%w TMPC/PS blends at 242 °C of each theory.

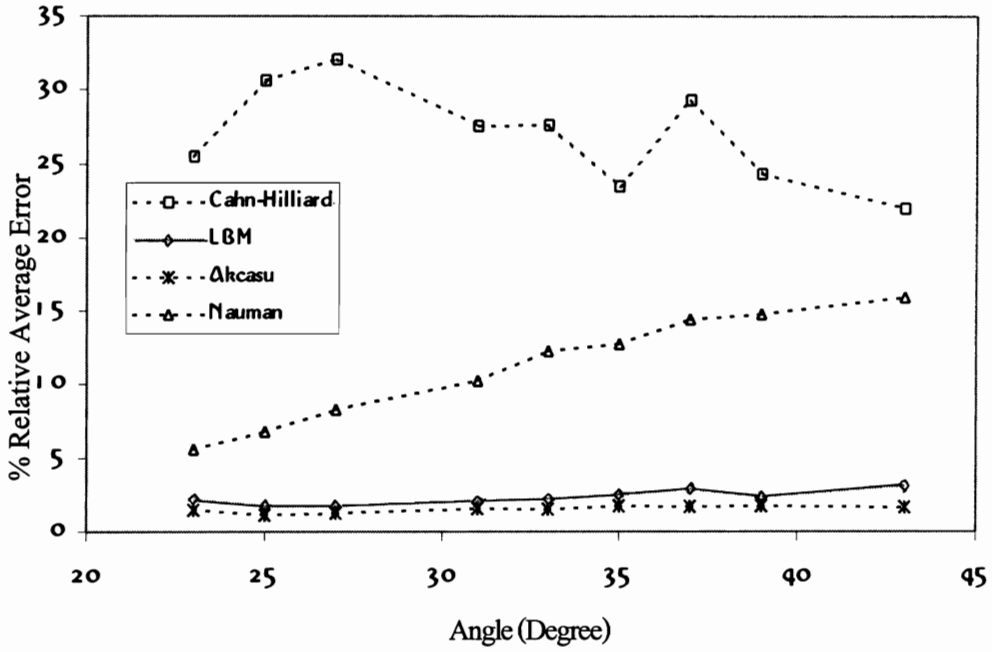

Figure 24 The percent relative average error of 50%w TMPC/PS blends at 293°C of each theory.

Conclusions

The present work involved studying the uses of various theories of spinodal decomposition to describe the same experimental results on the phase separation of polymer blends. Comparisons of calculated data theories and experimental data were made. From this method, the best theory, which can be used to describe the experimental results can be found. The number of conclusions from the results of this work can be summarized as follows:

1. Akcasu, *et al.* (1992) theory seems to be the best fitted theory that can be used to fit with selected experimental results. This might be the result from the $Z(q,t)$ factor.

2. Nauman, *et al.* (1994); and Cahn, *et al.* (1971) theories are in good agreement with experimental results at the beginning of the spinodal decomposition process.

3. The percent relative average errors increase with increasing temperatures. It is suggested that the four theories can be used to predict the spinodal decomposition process at a low quench depth. For deeper quench depth inside the unstable phase separation regime, the differences between the values calculated from theories and experimental values are larger.

4. The temperatures will incline to influence the fitted testing data, and at low temperatures the data can fit with the experimental results better than at higher temperatures.

Nomenclature

a(x,t)	Mole fraction of Nauman and Balsara (1989) theory
A(t)	The high order term of Free energy of Langer, *et al.* (1975) theory
a, b, c, d (equation 2.3)	Coefficients of Langer, *et al.* (1975) theory
a', b', c', d' (equation 2.6)	Coefficients of Langer, *et al.* (1975) theory
A, B, C, D(equation 2.7)	Total coefficients of Langer, *et al.* (1975) theory
A', B', C', D'(equation 3.5)	Coefficients of Akcasu, *et al.* (1992) theory
A''', B''	The expansion terms of Nauman and Balsara (1989) theory
C(q)	Nonlinear term
D_{AB}	Diffusion coefficient
E	Intensity factor
f, h, j, l (equation 4.18)	Coefficients of Nauman and Balsara (1989) theory
f', h', j', l' (equation 4.19)	Coefficients of Nauman and Balsara (1989) theory
g''	The second derivative of free energy
I(q,t)	Scattered intensity
I_{EXP}	Experimental data
I_{Th}	Calculated data of each theory
K	Gradient energy
M	Mobility
n	Refractive index of the blend
PS	Polystyrene
q	Scattering wave vector
q_c	Critical value of q
R(q)	The q dependent growth rate
S(q,t)	Structure function
$S_x(q)$	Structure function at the equilibrium
t	Time
T	Temperature
TMPC	Tetra methyl Bisphenol A polycarbonate
Z(q,t)	Chain connectivity function of Nauman and Balsara (1989) theory
κ	Compressibility
λ	Wavelength of the radiation
θ	Scattering angle

References

Akcasu, A. Z., Bahar, I., Erman, B., Feng, Y. and Han, C. C. 1992. Theoretical and experimental study of dissolution of inhomogeneities formed during spinodal decomposition in polymer mixtures. *J. Chem. Phys.* **97(8)** : 5782-5793.

Binder, K. 1983. Collective diffusion, nucleation, and spinodal decomposition in polymer mixtures. *J. Chem. Phys.* **79(12)** : 6387-6409.

Cahn, J. W. 1971. On spinodal decompostion. *Acta Metallurgica.* **9** : 795-801.

Cahn, J.W. and Hilliard, J. E. 1971. Spinodal decom position. *Acta Metallurgica.* **19** : 151-161.

Gennes, P. G. 1980. Dynamics of fluctuations and spinodal decomposition in polymer blends. *J. Chem. Phys.* **72(9)** : 4756-4763.

Langer, J. S., Bar-on, M. and Miller, D. 1975. New computational methods in the theory of spinodal decomposition. *Phys. Rev. A.* **11(4)** :1417-1429.

Nauman, E. B. and Balsara, N. P. 1989. Phase Equilibria and The Landau-Ginzburg Functional. *Fluid Phase Equilib.* **45** : 229-250.

Nauman, E. B. and He, D. Q. 1994. Morphology predictions for ternary polymer blends undergoing spinodal decomposition. *Polymer.* **35(11)** : 2243-2255.

Thongyai, S. 1990. *Determination of Polymer Miscibility by Calorimetry (First Year Report).* Ph.D. diss, Department of Chemical Engineering, London, Imperial College.

Thongyai, S. 1994. *Properties of Miscible and Phase Separated Polymer Blends.* Ph.D. diss, Department of Chemical Engineering, London, Imperial College.

Wang, Z.Y., Konno, M. and Saito, S. 1993. Kinetics of phase separation in polymer blends. (Calculations based on nonlinear theory). *J. Polym. Sci. : Part B: Polym. Phys.* **31** : 461-466.

(Revised version accepted December 24, 2001)